FIBER-OPTIC CURRENT SENSOR VALIDATION WITH TRIGGERED LIGHTNING MEASUREMENTS

Truong X. Nguyen, Jay J. Ely and George N. Szatkowski
NASA Langley Research Center
Hampton, VA 23681 U.S.A.
truong.x.nguyen@nasa.gov

Carlos T. Mata and Angel G. Mata
ESC - Kennedy Space Center, FL 32899 U.S.A.

Gary P. Snyder
NASA Kennedy Space Center, FL 32899 U.S.A.

ABSTRACT

A fiber optic current sensor based on the Faraday Effect is developed that is highly suitable for aircraft installation and can measure total current enclosed in a fiber loop down to DC. Other attributes include being small, light-weight, non-conducting, safe from electromagnetic interference, and free of hysteresis and saturation. The Faraday Effect causes light polarization to rotate when exposed to a magnetic field in the direction of light propagation. Measuring the induced light polarization rotation in fiber loops yields the total current enclosed.

Two sensor systems were constructed and installed at Camp Blanding, Florida, measuring rocket-triggered lightning. The systems were similar in design but with different laser wavelengths, sensitivities and ranges. Results are compared to a shunt resistor as reference. The 850nm wavelength system tested in summer 2011 showed good result comparison early. However, later results showed gradual amplitude increase with time, attributed to corroded connections affecting the 50-ohm output termination. The 1550nm system also yielded good results in the summer 2012. The successful measurements demonstrate the fiber optic sensor's accuracies in capturing real lightning currents, and represent an important step toward future aircraft installation.

ACRONYMS AND SYMBOLS

(a),(b),(c): Detector output voltages
A : Ampere
B : Magnetic flux density
c : Speed of light
CT : Current Transformer
DC : Direct-current
E : Polarization
H : Magnetic field
I : Enclosed current
L : Fiber interaction length
msec: Millisecond
MM: Multi-mode
n : Index of refraction
N : No. of closed fiber loops
PM : Polarization-maintaining (fiber)
SM : Single-mode
SLD: Superluminescent diode
t : Transit time
V : Verdet constant
ϕ : Polarization Rotation angle
μ_o : Free space permeability

INTRODUCTION

Growing applications of composite materials in commercial aircraft manufacturing have significantly increased the risk of aircraft damage due to lightning attachment. A risk mitigation strategy involves determining lightning current intensities and distributions on the aircraft from which damage risks could be inferred. Suitable onboard current sensors can be used to measure current intensities and paths during a strike.

For aircraft lightning current measurement, it is desirable to have a current sensor that measures total lightning current directly (not its time derivative), operates down to (near) DC frequency, conforms to aircraft structure, has large dynamic range, and is light-weight and safe (non-conductive). These characteristics cannot all be achieved with traditional sensors such as B-Dot sensors, I-Dot sensor and Rogowski coil variants. I-Dot and B-Dot sensors, for measuring the time derivatives of the current (I) and magnetic field (B), were used on the NASA F-106 in the Storm Hazard Program in the 1980's [1]. Output from these sensors must be integrated to yield desired parameters, and accuracy is a concern at very low frequencies where most of the lightning energy is concentrated. Ferromagnetic-core

current transformers are self-integrating and can measure current directly. However, aircraft applications are limited due to the large size, weight, and the tendency to saturate in strong currents or magnetic fields. Solid state current sensors based on Hall Effect, giant magnetoresistance and anisotropic magnetoresistance are often restricted to low bandwidth (up to a few hundred kilohertz) and must be protected from strong fields and currents. A shunt resistor can faithfully measure lightning waveforms, but it requires aircraft structure modifications to provide isolation between the terminals. I-Dot sensors, Rogowski coils, ferrite current transformers and shunt resistors can measure the total current, while others can only measure local current or magnetic field. These sensors typically require fiber optic converters to protect from hazards to personnel and instrumentation inside the aircraft. It is clear that each traditional sensor can satisfy only a few of the desirables previously listed.

Optical current sensors have been under development for decades. They are beginning to be commercialized, mostly to the power generation and distribution industries. The sensors typically rely on Faraday rotation in which the light's polarization plane rotates when its propagation medium is exposed to a magnetic field. The amount of rotation depends on the medium, the wavelength, and is proportional to the interaction length and the intensity of the magnetic field component in the direction of light propagation.

There are two main groups of optical sensing elements: crystal/bulk-glass based and fiber based. Crystal/bulk-glass based sensors can choose from an extensive list of available materials with wide ranges of optical properties. They can have high bandwidth, small size and be immune to vibration. They generally measure only local current or magnetic fields. This type of sensor has been proposed for lightning sensing on windmill structures [2].

The sensor discussed in this paper is optical fiber based. This sensor type is highly flexible, and by forming closed loop(s) around a structure, the enclosed current can be measured. Fig. 1 illustrates fiber loops measuring total lightning current flowing through aircraft structures of interest. By comparing amplitudes and timings at different locations, current flow paths may be determined. In contrast, the dots in the same

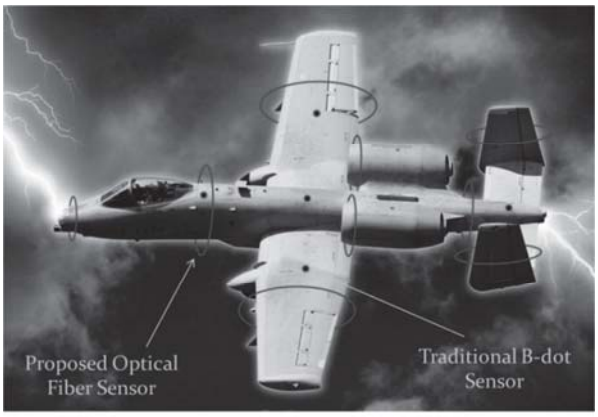

Fig. 1. Illustration of fiber optic current sensor on aircraft.

figure illustrate traditional field sensors, such as B-Dot, for sampling local B-fields. An inverse problem must be solved for the specific aircraft to approximate total current amplitudes [1,3].

There are many important advantages of a fiber optic current sensor over traditional sensors for aircraft lightning measurement. These include the abilities to conform to large, complex structure geometries. It is self-integrating, thus the output is directly related to the total current. The sensor is also small, lightweight, immune from interference, and free of hysteresis and saturation. The sensing fiber does not conduct electricity, and can be routed directly into the aircraft cabin without hazard to passengers and crews.

The sensor is highly suitable for applications such as in-flight lightning parameters characterization and can enable inferred damage assessments after a lightning strike. In addition, it can also be used to measure current internal to aircraft fuselage and other structures such as wing, with applications in system health monitoring or lightning transfer function certification purposes. Use on lightning towers and windmill structures is also possible.

The material choice for optical fiber is limited - most commonly available fiber materials are based on silica. The Faraday Effect in silica is weak, which makes it ideal for large currents in lightning. Temperature and bend/vibration sensitivities could be of concern depending on designs. The fiber is also fragile and needs suitable protection.

In the remainder of the paper, basic sensor operation, design, and bandwidth and some laboratory results are discussed. Finally, results

from field evaluations measuring rocket-triggered lightning current are presented. The Faraday rotation fiber optic current sensor is simply referred to as *Faraday sensor* in this paper.

FIBER-OPTIC CURRENT SENSOR SOLUTION

Due to the Faraday Effect, light polarization in an optical medium rotates when the medium is exposed to a magnetic field in the direction of light propagation. The amount of rotation depends on the material and the strength of the magnetic field component in the propagation direction. The effect in the fiber is illustrated in Fig. 2. The polarization plane rotation angle is given as [4]:

$$\phi = V \int \boldsymbol{B} \cdot d\boldsymbol{l} = \mu_0 V \int \boldsymbol{H} \cdot d\boldsymbol{l}\,, \tag{1}$$

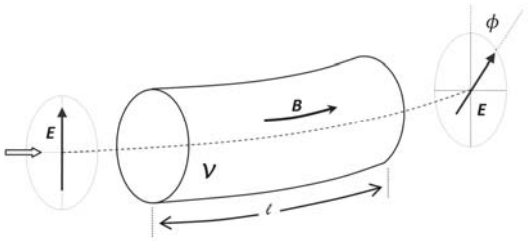

Fig. 2. Faraday Effect in optical fiber.

where μ_0 is the free-space permeability; V is the Verdet constant in radians/(meter·Tesla); $\mu_0 V$ is the combined permeability Verdet constant (radians/ampere); $\boldsymbol{B}$ is magnetic flux density in Tesla (T); length $\boldsymbol{l}$ (in meters) is the light and magnetic field interaction path length; and $\boldsymbol{H}$ is the magnetic field (amperes/meter). For a fiber forming N closed loops around a conductor carrying current **I** (ampere), applying Ampere's law yields

$$\phi = \mu_0 V \oint \boldsymbol{H} \cdot d\boldsymbol{l}\,, \\ = \mu_0 VNI\,. \tag{2}$$

Thus, the rotation angle is directly proportional to the current and the number of loops. Measuring the rotation angle can directly result in current. It is noted that the sensor is self-integrating, and no additional integration is needed.

Two sensor systems were developed; one operates at 850nm laser wavelength while the other at 1550nm. They are similar in design, but have different sensitivities and ranges from the different wavelengths. Both measure the induced rotation angle from which current can be determined. They are based on a reflective polarimetric scheme described below.

SENSOR DESCRIPTION

The measurement scheme for both systems is illustrated in Fig. 3. The scheme measures the polarization change induced by current. A linearly polarized light from a super-luminescence diode (SLD) laser is generated at locations labeled *1*, *2*. Half of the power is transmitted through the non-polarizing beam splitter (NBS) at *3* to the sensing fiber at *4*. The sensing fiber forms closed loops around the current carrying conductor at *5*. A Faraday mirror at *6* rotates the reflected light polarization by 90º relative to the incident light. This helps cancel fiber bend/stress induced effects makes the sensor less sensitive to bending. The reflected light traces back through the fiber to *3*, at which half of the power is reflected through the half-wave plate (HWP) at *7* toward the polarizing beam splitter (PBS) at *8*. Exiting the PBS, light power in the two orthogonal polarizations are measured by two photo-detectors D1 and D2 at *9*. The HWP helps rotate and align the initial polarization incident on the PBS. Ideally, at zero current the incident polarization should be at 45º relative to the PBS's two orthogonal principle polarization axes, so that beam power is divided equally between the two optical detectors at *9*. A balanced detector, with two built-in matched detectors, is used in place of two separate detectors. This helps subtract common-mode noise between the two detectors and improves overall noise performance.

This setup is referred to as a reflective scheme, since a mirror is used. Using this scheme in combination with a Faraday mirror, as light travels

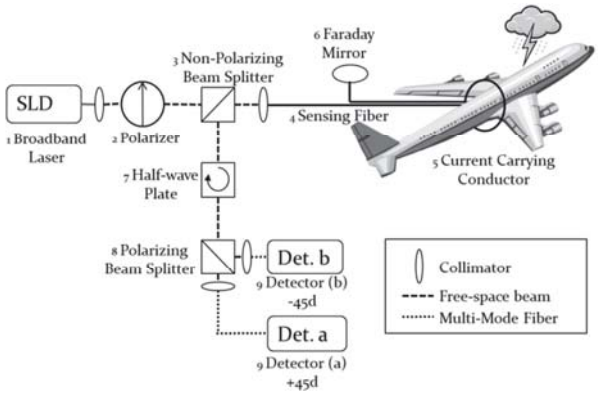

Fig. 3. Reflective polarimeric scheme with dual detectors.

through the fiber twice the non-reciprocal Faraday rotation due to current is doubled while stress induced effects are subtracted [5].

The responses at the two detectors should ideally be $(a),(b)=0.5*(1\pm sin(4\mu_0 VNI))$ for reflective scheme. Mathematic operation *difference-over-sum*, $(c) = \frac{(a-b)}{(a+b)}$, yields

$$(c) = \sin(4\mu_0 VNI), \text{ or} \quad (3)$$

$$NI = \frac{1}{4\mu_0 V}\sin^{-1}(c), \quad (4)$$

where *NI* is the number of loops *N* times the current *I*, and $\mu_0 V$ = 2.5x10^{-6} rad/A at 850nm and 0.718x10^{-6} rad/A at 1550nm [4]. The difference operation is actually performed with the balanced detector that yields only one voltage waveform output. The sum operation is performed separately and does not change with current.

Two different sensing fibers are used in the two setups. A 50m long *twisted* fiber is used in the 850nm system. It is made from a standard single-mode (SM) telecom fiber that is twisted at 20 twists per meter. Twisting helps hold the state-of-polarization otherwise would be destroyed in a typical single-mode fiber. The 1550nm system uses a 25m-long *spun* polarization-maintaining (PM) fiber [6]. Spun PM fiber is the result of twisting a PM fiber during manufacturing. The twist (or spun) rate is about 3mm per turn.

Fig. 4 describes ideal responses at the two wavelengths. The curves labeled (a) and (b) are from the two optical detectors. While either can be used to determine current, performing difference-over-sum operation $(c) = \frac{(a-b)}{(a+b)}$ would yield a response that is more sensitive (higher slope), with zero crossing at zero current, and has larger dynamic range due to the common-mode noise subtraction. Current is computed from (*c*) using eq. (3).

The typical operating range is in the region where curves [*c*] increases monotonically in Fig. 4, or about -160 kA to +160 kA for the 850nm system, and -500 kA to +500 kA for the 1550nm system. Non-ideal medium and components in a practical system will distort the curves, and the ranges will be slightly reduced.

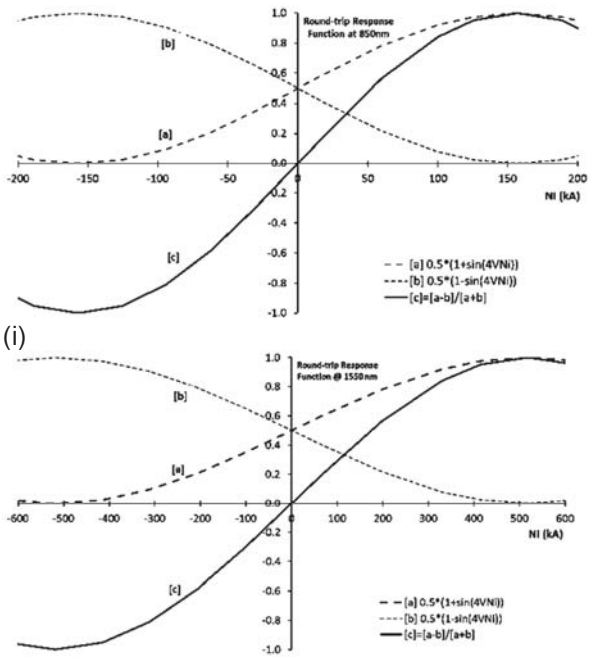

(i)

(ii)

Fig. 4. Ideal sensor responses at 850nm and 1550nm optical wavelengths.

Sensor Response and Data Correction

The two systems were measured in laboratory against reference sensors that include a Rogowski coil (with an electronic integrator), and a ferrite-based Pearson™ current transformer (CT). Fig. 5 and 6 compare the three sensors by plotting current from the Faraday sensors on the vertical axis against current from other reference sensors on the horizontal axis. The Faraday sensors' outputs are computed using (3).

In perfect setups, the Faraday sensor data would fall on the straight diagonal lines labeled as "ideal" in the figures. In practice, the data to follow curves labeled "uncorrected". The lower slopes in the linear region near zero current indicated reduced sensitivities than ideal. In addition, the curves become non-linear at higher current amplitudes. This deviation from linear is the result of light depolarization caused by non-ideal optical components and fiber medium. Additional details characterizing light propagation in the fiber can be found in [6-11].

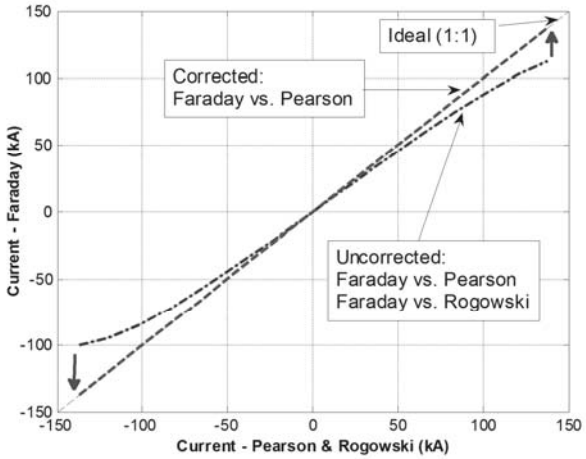

Fig. 5. The 850nm system's response curve, corrected and un-corrected.

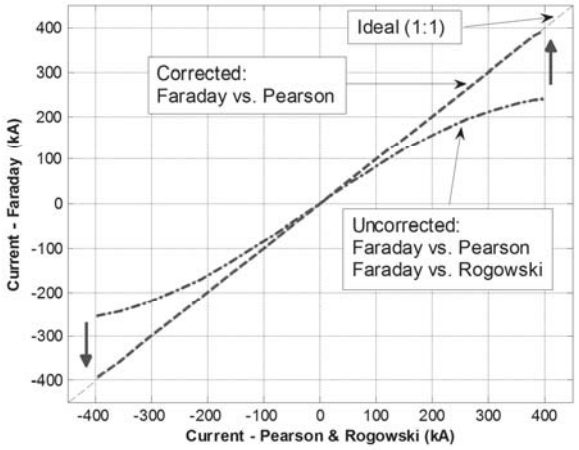

Fig. 6. The 1550nm system's response curve, corrected and un-corrected.

To correct for both the reduced sensitivity and the non-linear response, simple spine-fit "correction" functions are developed from each of Fig. 5 and 6 that map the Faraday sensor response to the "ideal" curves. The "corrected" response curves align well with the ideal diagonal lines shown in the same plots. These same correction functions can then be applied to subsequent measurements to achieve correct results. An alternative to curve-fitting is interpolation. Neither approach is perfect, as some small error may remain.

Fig. 7 illustrates the "uncorrected" and "corrected" Faraday sensor data against the reference sensors for a 100 kA peak current waveform using the 850nm system. Good comparison against reference sensors was achieved after the correction. It is noted that in these tests, optical

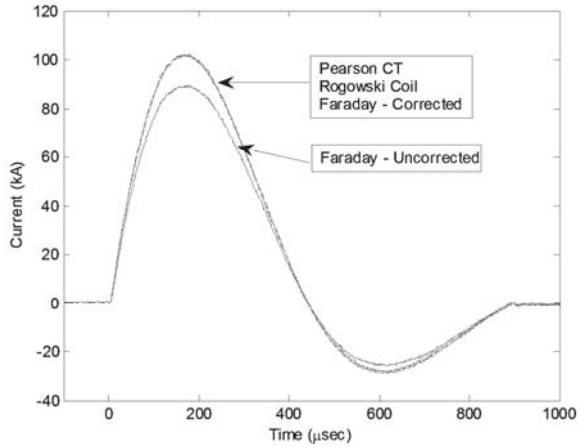

Fig. 7. Good comparison with reference sensor achieved after correction. N*I= 100 kA.

effects associated with high currents are produced using a multi-turn current coil to increase magnetic field and/or with multiple fiber loops to multiply the optical effects. For Fig. 7, a 100-turn coil and one fiber loop were used. Additional details have been previously discussed in [12-14].

Sensor Bandwidth

Bandwidth of a sensor system is limited by the lowest bandwidth of its components. For the fiber sensor component, it is limited by the light transit time in the interaction length of the fiber. This bandwidth limitation is to ensure the total transit time is much faster than the signal change rate. The fiber interaction length in the bandwidth consideration includes the round-trip length around the conductor and includes the length to and from the Faraday sensor. The 3-dB sensor bandwidth (BW) is [4,5]: $BW \approx \frac{0.44}{t} \approx 0.44c/nl$, where t is transit time, c is the speed of light in free space, n is the index of refraction in fiber material (n=1.5), and l is the interaction length (double of fiber length for the reflective scheme described).

Table 1 computes the maximum fiber length and structure dimensions for different bandwidths. Aircraft thin structures may include wings and tail surfaces, while round structures may include fuselage, engine, etc. For reference, fuselage outside diameters for various aircraft (averaging the width and height) include: Airbus A380: 7.8 m; Boeing 767: 5.3 m; Boeing 737: 3.8 m. Assuming most of the damaging lightning energy is contained in spectrum far below 1-2 MHz, the

table shows there is sufficient sensor bandwidth even for the fuselage of the largest passenger aircraft, the Airbus A380.

Table 1. Dimension vs. Sensor Bandwidth

3-dB Bandwidth (MHz)	Max. Fiber Length (m)	Thin Structure Dimension (m)	Round Structure Diameter (m)
1	44	22	14
2	22	11	7
4	11	5.5	3.5
10	4.4	2.2	1.4
20	2.2	1.1	0.7

TRIGGERED-LIGHTNING SETUP

Over the summers of 2011 and 2012, the sensor systems were evaluated measuring rocket-triggered lightning at the International Center for Lightning Research and Testing (ICLRT) facility in Camp Blanding, Florida [15]. In the setup (Fig. 8 background), triggered lightning flashes would attach to the wire cage, and the currents would travel to the ground via a shunt resistor (T&M Model R-7000-10) and a down-conductor. A part of the sensing fiber formed closed loops around the conductor as shown in Fig. 9. The remaining fiber segments at the two ends were co-routed radially away from the site. One end was connected to the optical box 12m away near the digitizers for data acquisition. The other end was connected to a Faraday mirror that was buried in the ground to minimize temperature variations. Due to insufficient fiber length in the 1550nm system, the Faraday mirror was only about 1/3 the distance (4m) from the launch tubes. Thus, approximately an 8m section of the sensing fiber was "unpaired", and potentially subjected to effects from ground current. By routing the fiber radially away from the lightning tower, the magnetic field component parallel to the fiber is expected to be minimized, lessening undesirable effects from ground current. The fibers were protected inside combinations of rain gutters, garden hose (850nm fiber) or plastic braided sleeves (1550nm fiber) to protect from wild animals or being trampled on.

Data for both the Faraday sensors and the shunt resistor were recorded using 14-bit digitizers sampled at 100 mega-samples per second. The sensors and the digitizers were powered by batteries.

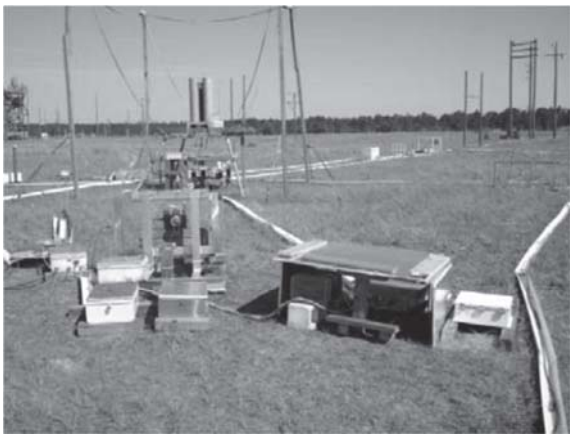

Fig. 8. Measurement setup for the 850nm system. Rocket launch tubes can be seen at distance 12m away in the background. The optical box is under the shelter in the lower right

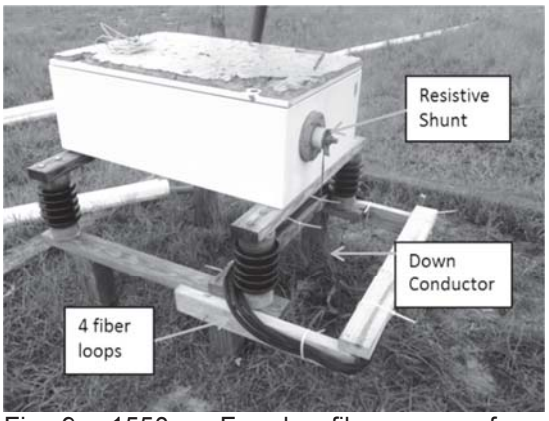

Fig. 9. 1550nm Faraday fiber sensor forms four loops around the lightning down conductor. Reference shunt resistor is in box above.

RESULTS FOR 850NM BASED SYSTEM

During May – August 2011, data for nine lightning flashes were captured – each flash typically contained more than one stroke. The results from the first flash compared very well against the reference resistive shunt. Fig. 10 shows the result for one of the five strokes in the first flash captured. Current down to 100A could be observed in many recorded waveforms. Additional data can be found in [13]. The good result demonstrates the measurement accuracy and feasibility in a real lightning environment. The Faraday sensor data were slightly smoothed for noise reduction.

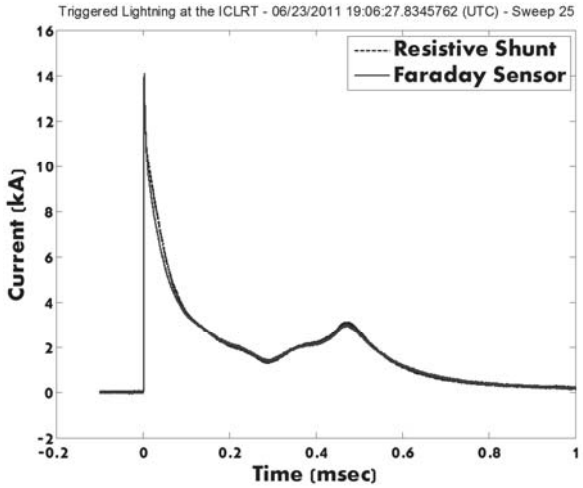

Fig. 10. Triggered lightning current measured with Faraday sensor versus shunt resitor

Subsequent measurements, however, showed amplitude increases relative to the shunt resistor that gradually became worse with time. To match amplitudes, the Faraday sensor data had to be numerically scaled down. The multiplicative scale factor was 0.9 for the measurements two weeks after the first data set and gradually decreased to 0.72 at the end of the summer. The suspected cause was connector corrosion in the cable connecting to the data acquisition system (made of two short cables partially exposed to the weather). The contact resistance caused the termination impedance to rise beyond the normally 50-ohm value, thus the amplified amplitudes as the result. When the magnitudes were scaled to similar level, the waveforms compared very well. Fig. 13 shows the comparison of data from the second flash recorded 2 weeks later. The Faraday sensor data were scaled down to 90% in this comparison. Both the digitizers and the Faraday sensor performed well when retrieved and tested at the end of the season.

RESULTS FROM THE 1550nm SYSTEM

Before any triggered lightning measurements were conducted in the summer 2012, a series of tests were conducted comparing the outputs from three different sensors: the 1550nm-based Faraday sensor, the reference shunt resistor, and a ferrite-based current transformer. In these tests, one kA positive and negative current waveforms were injected onto the wire cage surrounding the rocket launch tubes while the return current was extracted at the base of the down-conductor. Though not shown here the results compared very

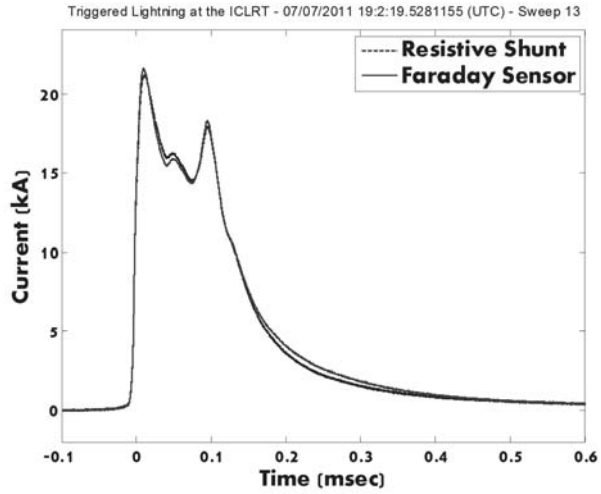

(i)

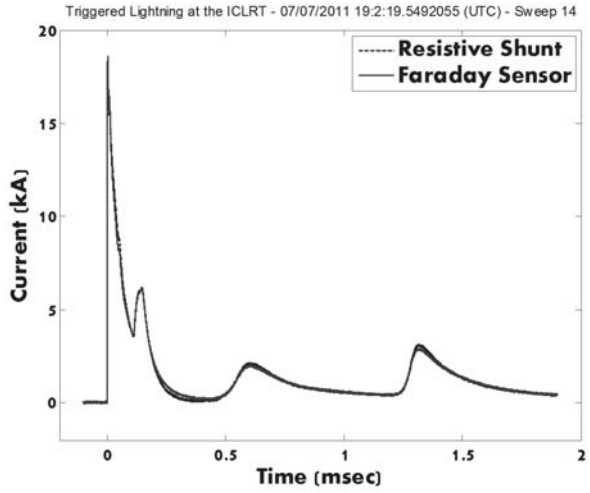

(ii)

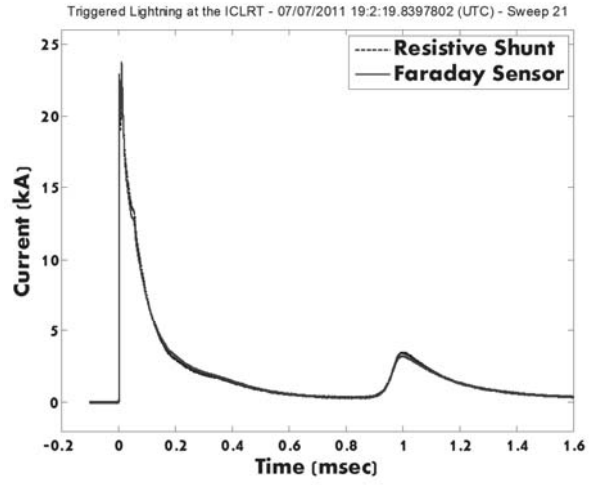

(iii)

Fig. 11. Sample stroke data for the 850nm system two weeks after the first flash. Data amplitudes were reduced to 90% for comparison with resistive shunt data.

well, thus the operation of the Faraday sensor was verified. It is noted that there was no ground current in this test setup as with actual lightning flashes.

Early results showed the system suffered electromagnetic interference due to strong ground currents. Interference was evidenced by detector output components (a) and (b) not being symmetrical to one another (see Fig. 4). In later measurements, interference became much less simply by raising the data cables between the optical box and the data acquisition system slightly off the ground (about 5 cm above the ground, supported underneath by a wood beam). Fig 12 illustrates good comparisons with the shunt resistor were achieved. Electric current amplitude-versus-time waveforms are nearly identical between the two sensors. The long time-scales chosen highlight the sensor's ability to measure long duration components, including continuing current.

ADDITIONAL OBSERVATIONS

Upon close data examination, interference from ground current on the data cables was still evident in both the 850nm and the 1550nm setups. Initial peak current values were affected by up to about 400A. The problem was confirmed when the Faraday sensor system accidentally turned off; lightning induced pulses were seen at the digitizers, having peaks equivalent of up to about 400A. In addition, the pulses' timings corresponded with the peaks of the lightning strokes. It is believed that raising the cables even higher off the ground than the existing 5 cm could make the measurements even more accurate.

Both the cable corrosion and the ground current interference problems could be minimized in future setups by having better cable and box shielding, by elevating the setups higher above the ground, or by having the optical box and the digitizers in the same shielded enclosure. It is noted that the same issues are not of concern for aircraft installations because instruments will be located inside the aircraft cabin.

CONCLUSION

Good result comparisons were achieved between the Faraday fiber optic current sensors and the reference shunt resistor measuring triggered lightning. This demonstrates the accuracy and feasibility of using the Faraday sensor for lightning

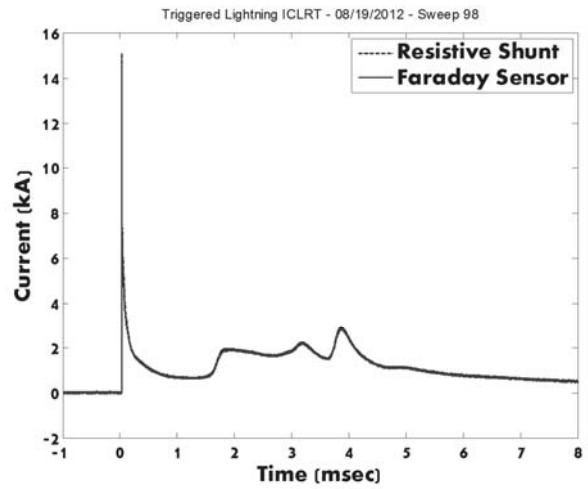

(i)

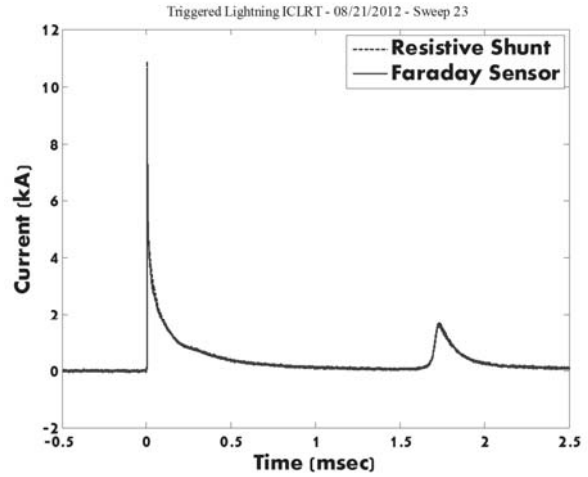

(ii)

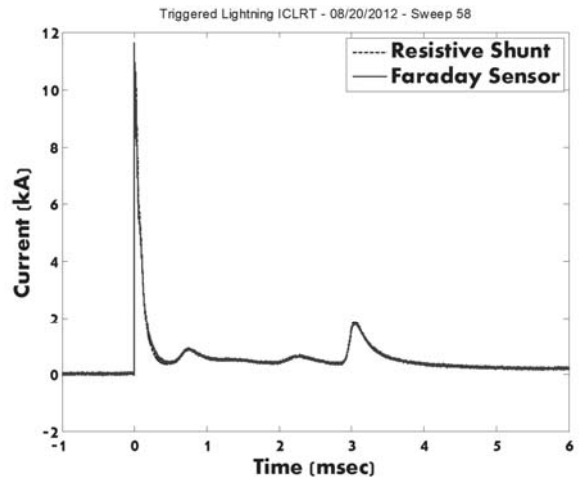

(iii)

Fig. 12. Three results for the 1550nm system show good comparison with resistive shunt.

current measurement in a real lightning environment. Along with other important and unique characteristics of fiber optic sensor, the results represent an important step toward aircraft installation.

REFERENCES

[1] F. L. Pitts, B. D. Fisher, V. Mazur, and R. A. Perala, "Aircraft Jolts from Lightning Bolts," IEEE Spectrum, July 1988.

[2] S. G. M. Krämer, and F. P. León, "Fiber-Optic Current Sensors for Lightning Detection in Wind Turbines," OSA/OFS, 2006.

[3] S. Alestra, I. Revel, V. Srithammavanh, M. Bardet, R. Zwemmer, D. Brown, N. Marchand, J. Ramos, V. Stelmashuk, V. "Developing an In-Flight Lightning Strike Damage Assessment System," ICOLSE, 2007.

[4] J. M. Lopex-Higuera, Editor. Handbook of Optical Fibre Sensing Technology, 2002; Sections 27.2 - 27.4.

[5] P. Drexler and P Fiala,"Utilization of Faraday Mirror in Fiber Optic Current Sensors", Radioengineering, Vol. 17, Dec. 2008

[6] R.I. Laming and D.N. Payne, "Electric Current Sensors Employing Spun Highly Birefringent Optical Fibers," Journal of Lightwave Technology, Dec. 1989.

[7] A. M. Smith, "Polarization and Magneto-optic Properties of Single-Mode Optical Fiber," Applied Optic, Jan. 1978.

[8] R. Ulrich, and A. Simon, "Polarization Optics of Twisted Single-Mode Fibers," Applied Optics, Vol. 18, Issue 13, pp. 2241-2251 (1979).

[9] S. C. Rashleight, "Origins and Control of Polarization Effects in Single-Mode Fibers," Journal of Lightwave Technology, Vol. LT-1, No. 2, 1983.

[10] G. W. Day, and A. H. Rose, "Faraday Effect Sensors: The State of the Art," Proc. SPIE, 1988, pp. 138–150.

[11] A.D. White, G.B. McHale, D.A. Goerz, "Advances in Optical Fiber-Based Faraday Rotation Diagnostics," 17th IEEE Int. Pulsed Power Conference, Wash. DC, July 2009 (LLNL-CONF-415198).

[12] T. X. Nguyen, and G. N. Szatkowski, "Fiber Optic Sensor for Aircraft Lightning Current Measurement", Int. Conf. on Lightning and Static Electricity (ICOLSE) 2011.

[13] T.X. Nguyen, J.J. Ely, G.N. Szatkowski, C.T. Mata, A.G Mata, and G.P. Snyder, "Fiber-Optic Sensor for Aircraft Lightning Current Measurement," Int. Conf. on Lightning Protection (ICLP), 2012

[14] T.X. Nguyen, J.J. Ely and G.N. Szatkowski, "A 1310nm-Based Fiber-Optic Sensor for Aircraft Lightning Current Measurement," ICOLSE 2013.

[15] V. A., Rakov, "A review of Triggered-Lightning Experiments," 30th International Conference on Lightning Protection, Cagliari, Italy, September 13-17, 2010.